of different tasks exhibited a null or negative correlation. This trend held across all tasks and subjects, as shown by Fig. 3E. These results are consistent with the hypothesis that transient cross-frequency coupling modulates network engagement, enabling flexible control of cognitive processing.

Oscillations are rhythmic fluctuations in neuronal excitability that modulate both output spike timing and sensitivity to synaptic input (*5*). Therefore, effective communication between neuronal populations requires precise matching of the relative phase of distinct rhythms to axonal conduction delays. An oscillatory hierarchy operating across multiple spatial and temporal scales could regulate this proposed long-range communication (*13*). Basal forebrain cortical-projecting GABAergic (γ-aminobutyric acid–releasing) neurons are well positioned to control theta/HG coupling; these neurons preferentially synapse onto intracortical GABAergic neurons throughout the cortex, with disinhibitory spike bursts causing a brief increase in gamma power at the theta trough (*28*). Our observations that (i) HG power is modulated by theta phase, (ii) an increase in theta power strengthens theta/HG coupling, and (iii) the topography of theta/HG coupling is task-dependent support the hypothesis that cross-frequency coupling between distinct brain rhythms facilitates the transient coordination of cortical areas required for adaptive behavior in humans.

References and Notes

1. G. Buzsaki, A. Draguhn, *Science* **304**, 1926 (2004).
2. K. Linkenkaer-Hansen, V. V. Nikulin, S. Palva, R. J. Ilmoniemi, J. M. Palva, *J. Neurosci.* **24**, 10186 (2004).
3. T. Womelsdorf, P. Fries, P. P. Mitra, R. Desimone, *Nature* **439**, 733 (2006).
4. J. P. Lachaux *et al.*, *Neuroimage* **25**, 491 (2005).
5. P. Fries, *Trends Cogn. Sci.* **9**, 474 (2005).
6. J. M. Schoffelen, R. Oostenveld, P. Fries, *Science* **308**, 111 (2005).
7. E. M. Izhikevich, *Neural Netw.* **14**, 883 (2001).
8. A. Bragin *et al.*, *J. Neurosci.* **15**, 47 (1995).
9. G. Buzsaki *et al.*, *Neuroscience* **116**, 201 (2003).
10. A. G. Siapas, E. V. Lubenov, M. A. Wilson, *Neuron* **46**, 141 (2005).
11. H. Lee, G. V. Simpson, N. K. Logothetis, G. Rainer, *Neuron* **45**, 147 (2005).
12. J. J. Chrobak, G. Buzsaki, *J. Neurosci.* **18**, 388 (1998).
13. P. Lakatos *et al.*, *J. Neurophysiol.* **94**, 1904 (2005).
14. A. D. Ekstrom *et al.*, *Hippocampus* **15**, 881 (2005).
15. P. B. Sederberg, M. J. Kahana, M. W. Howard, E. J. Donner, J. R. Madsen, *J. Neurosci.* **23**, 10809 (2003).
16. J. Onton, A. Delorme, S. Makeig, *Neuroimage* **27**, 341 (2005).
17. B. Schack, N. Vath, H. Petsche, H. G. Geissler, E. Moller, *Int. J. Psychophysiol.* **44**, 143 (2002).
18. J. M. Palva, S. Palva, K. Kaila, *J. Neurosci.* **25**, 3962 (2005).
19. P. L. Nunez, R. S. Srinivasan, *Electric Fields of the Brain: The Neurophysics of EEG* (Oxford Univ. Press, Oxford, 2005).
20. N. E. Crone, D. L. Miglioretti, B. Gordon, R. P. Lesser, *Brain* **121**, 2301 (1998).
21. E. Edwards, M. Soltani, L. Y. Deouell, M. S. Berger, R. T. Knight, *J. Neurophysiol.* **94**, 4269 (2005).
22. N. K. Logothetis, J. Pauls, M. Augath, T. Trinath, A. Oeltermann, *Nature* **412**, 150 (2001).
23. R. Mukamel *et al.*, *Science* **309**, 951 (2005).
24. J. Niessing *et al.*, *Science* **309**, 948 (2005).
25. Materials and methods are available as supporting material on *Science* Online.
26. M. J. Kahana, D. Seelig, J. R. Madsen, *Curr. Opin. Neurobiol.* **11**, 739 (2001).
27. R. Miller, *Cortico-Hippocampal Interplay and the Representation of Contexts in the Brain* (Springer-Verlag, New York, 1991).
28. S. C. Lin, D. Gervasoni, M. A. L. Nicolelis, *J. Neurophysiol.* (2006); doi: 10.1152/jn.00524.2006.

29. This work was supported by the Rauch family, National Institute of Neurological Disorders and Stroke grant NS21135, NSF Fellowship 2004016118, and National Institute on Deafness and Other Communication Disorders grant F31DC006762. The authors thank P. Garcia and D. Filippi of the Department of Neurology, University of California San Francisco, for their help on electrical stimulation mapping and localizing epileptic tissue.

Supporting Online Material

www.sciencemag.org/cgi/content/full/313/5793/1626/DC1
Materials and Methods
SOM Text
Figs. S1 to S8

30 March 2006; accepted 20 July 2006
10.1126/science.1128115

Caveolin-1 Is Essential for Liver Regeneration

Manuel A. Fernández,[1,2]* Cecilia Albor,[1]* Mercedes Ingelmo-Torres,[1] Susan J. Nixon,[2] Charles Ferguson,[2] Teymuras Kurzchalia,[3] Francesc Tebar,[1] Carlos Enrich,[1] Robert G. Parton,[2]† Albert Pol[1]†

Liver regeneration is an orchestrated cellular response that coordinates cell activation, lipid metabolism, and cell division. We found that *caveolin-1* gene–disrupted mice (*cav1*$^{-/-}$ mice) exhibited impaired liver regeneration and low survival after a partial hepatectomy. Hepatocytes showed dramatically reduced lipid droplet accumulation and did not advance through the cell division cycle. Treatment of *cav1*$^{-/-}$ mice with glucose (which is a predominant energy substrate when compared to lipids) drastically increased survival and reestablished progression of the cell cycle. Thus, caveolin-1 plays a crucial role in the mechanisms that coordinate lipid metabolism with the proliferative response occurring in the liver after cellular injury.

The liver is pivotally positioned in the regulation of the body's metabolic homeostasis of lipids, carbohydrates, and vitamins. In addition, it produces essential serum proteins, lipoproteins, enzymes, and cofactors. Paradoxically, the liver is also the main detoxifying organ in the body, being continuously exposed to the threat of cellular injury. Consequently, the liver has evolved complex regenerative mechanisms to respond to chemical, traumatic, or infectious injuries (*1*–*3*). During regeneration, the liver continues to accomplish its critical functions, such as glucose homeostasis, protein synthesis, and bile secretion. Liver regeneration does not require stem cells but instead occurs when differentiated and largely quiescent hepatic cells reenter the cell cycle to replace the lost functional mass.

One of the most extensively characterized model systems to study liver regeneration is the partial hepatectomy in rodents. In this model, the left and medial lobes of the liver are excised, resulting in removal of 70% of the hepatic mass. Within minutes, hepatocytes then undergo a coordinated cellular activation termed the acute phase response. This highly regulated process is simultaneously mediated by different growth factors and cytokines that conduct the response signal into kinases and transcription factors. As a result of the acute response, the hepatocyte initiates the transcription of more than 100 early genes, accumulates triacylglycerol and cholesterol esters in intracellular lipid droplets (*4*), and progresses through the cell cycle. Lipid droplet formation is an essential part of the proliferative response during liver regeneration (*5*). Lipids stored in lipid droplets are delivered into the bile or used in the production of new lipoproteins and bile acids, for the synthesis of new membranes, or to supply the energy required for remnant hepatocytes to rebuild the liver. By compensatory hyperplasia, the regenerative process reestablishes the original liver mass in approximately 1 week, after which hepatocytes return to a quiescent state.

Caveolae are distinct domains of the plasma membrane of most cells, where cellular processes such as signaling and membrane sorting occur in a highly regulated lipid and protein environment (*6*). Caveolin, an essential component of caveolae, is a protein that has the distinct capability to create these highly ordered domains at the cell surface. In addition, caveolin and caveolae are key elements in the regulation of the intracellular homeostasis of lipids, cell activation, and cell

[1]Departament de Biologia Cellular, Facultat de Medicina, Institut d'Investigacions Biomèdiques August Pi i Sunyer, Universitat de Barcelona, Casanova 143, 08036 Barcelona, Spain. [2]Institute for Molecular Bioscience, Centre for Microscopy and Microanalysis and School of Biomedical Sciences, University of Queensland, Brisbane, Queensland 4072, Australia. [3]Max-Plank-Institute of Molecular Cell Biology and Genetics, Pfotenhauerstrasse 108, 01307 Dresden, Germany.

*These authors contributed equally to this work.
†To whom correspondence should be addressed. E-mail: R.Parton@imb.uq.edu.au (R.G.P.); apols@ub.edu (A.P.).

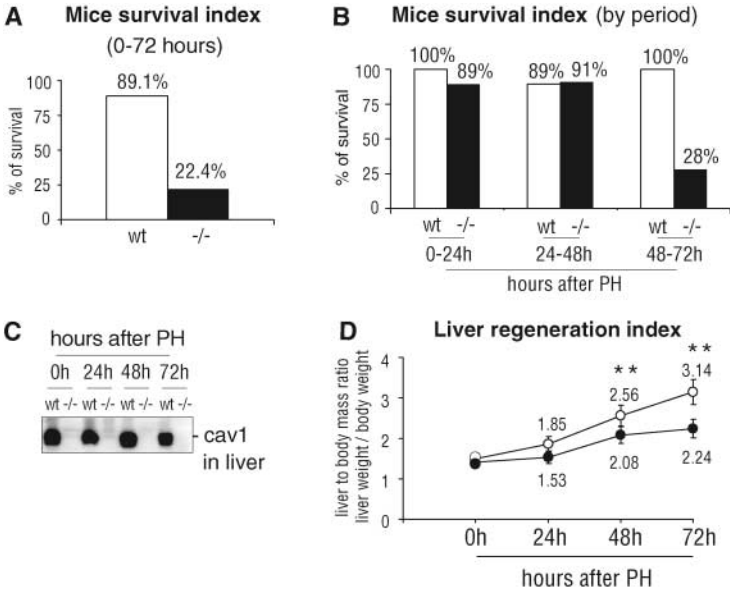

Fig. 1. Low survival and impaired liver regeneration of *cav1*$^{-/-}$ mice after partial hepatectomy. (**A**) Accumulated survival index 72 hours after partial hepatectomy of WT mice (white bars) and *cav1*$^{-/-}$ mice (black bars). (**B**) Survival index by period (0 to 24, 24 to 48, and 48 to 72 hours) of WT mice (white bars) and *cav1*$^{-/-}$ mice (black bars) for animals that, after partial hepatectomy (PH), reached and survived after each period. (**C**) Immunoblotting of caveolin-1 in liver homogenates corresponding to WT and *cav1*$^{-/-}$ mice after partial hepatectomy (40 μg of protein per lane). (**D**) Liver–to–body mass ratio in WT (white circles) and *cav1*$^{-/-}$ (black circles) animals. Immunoblots are representative of five independent experiments. The statistical significance of differences between WT and *cav1*$^{-/-}$ mice (asterisks) was determined with Student's *t* test, $^{**}P < 0.01$. Each point represents the average value and standard deviation of at least six independent measurements.

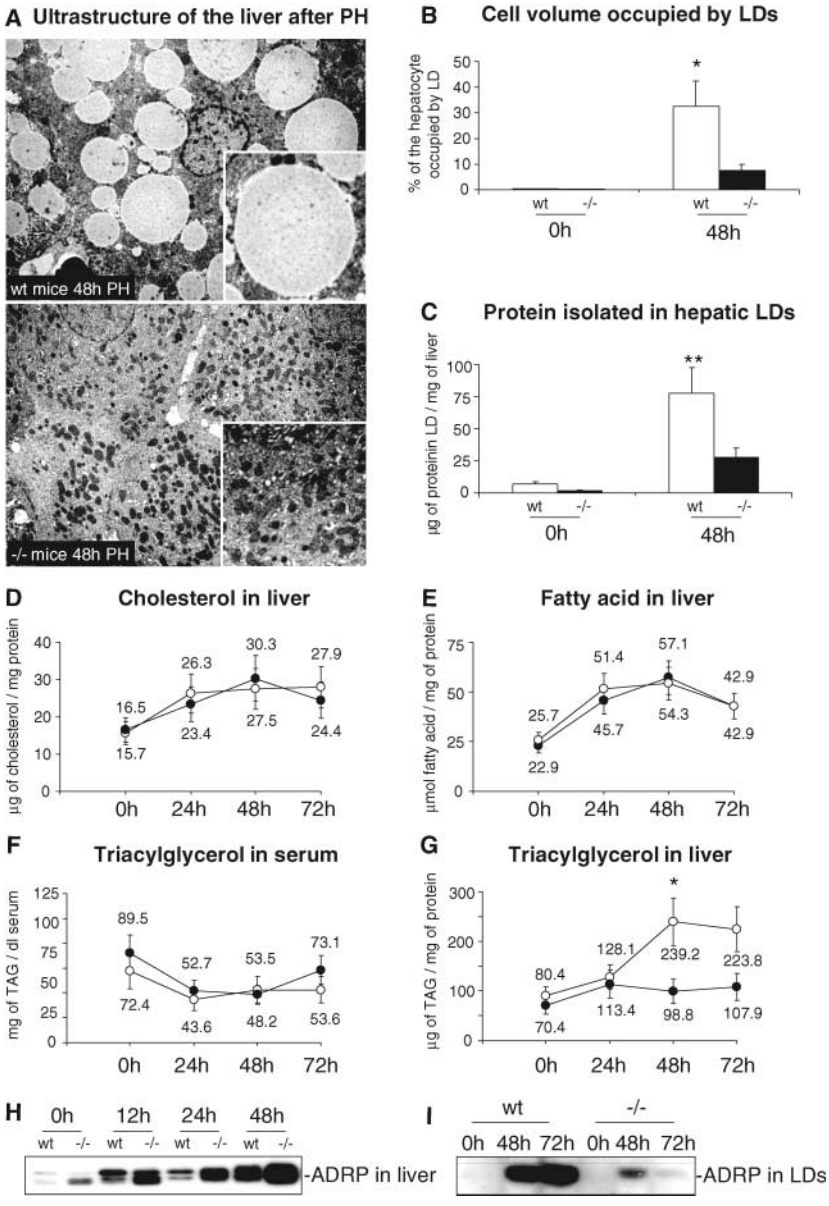

Fig. 2. Intracellular lipid imbalance in the liver of *cav1*$^{-/-}$ mice after partial hepatectomy. (**A**) Ultrastructure of the liver 48 hours after partial hepatectomy in WT mice (top panel) and *cav1*$^{-/-}$ mice (bottom panel). (**B**) Mean volume of the cell occupied by lipid droplets (LDs), calculated by quantitative EM, in WT mice (white bars) or *cav1*$^{-/-}$ mice (black bars) 48 hours after partial hepatectomy. (**C**) Amount of protein in a purified lipid droplet fraction from livers of WT mice (white bars) and *cav1*$^{-/-}$ mice (black bars). (**D** and **E**) Cholesterol and fatty acid levels in liver homogenates of WT mice (white circles) or *cav1*$^{-/-}$ mice (black circles) after partial hepatectomy. (**F** and **G**) Triacylglycerol levels in serum (F) and liver homogenates (G) of WT mice (white bars) and *cav1*$^{-/-}$ mice (black bars) after partial hepatectomy. (**H** and **I**) Expression of ADRP in liver homogenates (40 μg) (H) and lipid droplets purified from livers (30 μl) (G) of WT and *cav1*$^{-/-}$ mice. Immunoblots are representative of five (H) and two (I) independent experiments. The statistical significance of differences between WT and *cav1*$^{-/-}$ mice (asterisks) was determined with Student's *t* test, $^{*}P < 0.05$, $^{**}P < 0.01$. Each point represents the average value and standard deviation of at least four (B) or six [(C) to (G)] independent measurements.

proliferation. Recent work has linked caveolins to lipid droplet function (*7*). In addition, we have previously described the expression of caveolin and caveolae in hepatocytes and showed that caveolin associates with the lipid droplets formed after partial hepatectomy (*8*).

Liver regeneration results from the coordination of cell activation, lipid metabolism, and cell division. Although caveolin-1 has been connected with the regulation of each one of these processes, its precise role remains uncertain. Thus, the regeneration response triggered in the liver after partial hepatectomy offers an excellent integrated model system with which to evaluate in vivo the role of caveolin-1 in these processes occurring synchronously in a cell population. We studied the regeneration process triggered by partial hepatectomy in the liver of caveolin-1 gene–disrupted mice (*cav1*$^{-/-}$ mice) (*9*, *10*).

We analyzed 66 wild-type (WT) mice and 61 *cav1*$^{-/-}$ mice during the first 72 hours after partial hepatectomy. At the end of this period, WT mice showed an accumulated survival index of 89.1% (Fig. 1A). In contrast, *cav1*$^{-/-}$ mice showed a survival index of only 22.4%. Although the mortality of both groups was rather similar during the first 48 hours (100%/89% between 0 and 24 hours and 89%/91% between 24 and 48 hours for WT and *cav1*$^{-/-}$ mice, respectively), *cav1*$^{-/-}$ mice showed a marked mortality beyond this time point (72%) (Fig. 1B). In contrast, all of the WT mice that survived at 48 hours progressed to 72 hours. As expected, caveolin-1 was highly expressed in livers of WT mice but was not detected in *cav1*$^{-/-}$ mice at any point in the regeneration process (Fig. 1C). The liver–to–body mass ratio (equivalent to a regeneration index after partial hepatectomy), which was 5.9% in both untreated WT and *cav1*$^{-/-}$ mice, increased progressively in WT mice to reach 3.1% after 72 hours, which represents 52.5% of the original weight (Fig. 1D). Considering that only 22% of *cav1*$^{-/-}$ mice survived at this time point (Fig. 1A), the regeneration index of *cav1*$^{-/-}$ animals was 2.2% after 72 hours, which is only 38.0% of the original weight. *cav1*$^{-/-}$ mice that died during the period from 36 to 72 hours (78% of *cav1*$^{-/-}$ mice operated on) showed an extremely low regeneration index of approximately 1.7%.

After partial hepatectomy, the levels of fatty acids in the plasma increase severalfold, leading to intracellular accumulation of lipids and the formation of numerous cytosolic lipid droplets (*4*). We used quantitative electron microscopy (EM) to examine the ultrastructure of the liver after partial hepatectomy. No significant differences between WT and *cav1*$^{-/-}$ mice were observed in the serum (table S1) or liver before surgery; a small number of lipid droplets was observed in each case. Forty-eight hours after partial hepatectomy, the hepatocytes of WT mice accumulated enlarged lipid droplets in the cytosol (Fig. 2A). In contrast, lipid droplet accumulation was greatly reduced in the livers of *cav1*$^{-/-}$ mice. After 48 hours, the mean volume of lipid droplets was 32.6% (±9.8%) of cellular volume in WT mice as compared to 7.7% (±2.9%) in *cav1*$^{-/-}$ mice (Fig. 2B). When a purified fraction of lipid droplets was isolated from regenerating livers after 48 hours, a significant reduction in the total amount of purified protein from *cav1*$^{-/-}$ livers was observed (Fig. 2C). At this time, the levels of cholesterol and fatty acids in serum or in liver homogenates were not significantly different between WT or *cav1*$^{-/-}$ mice (Fig. 2, D and E), suggesting that a reduced level of serum lipids or reduced cellular uptake of lipids did not account for the lack of lipid droplets observed in the liver of *cav1*$^{-/-}$ mice. However, whereas the levels of triacylglycerol in serum were similar between WT and *cav1*$^{-/-}$ animals, the level of triacylglycerol in liver homogenates was clearly lower in *cav1*$^{-/-}$ animals after 48 hours (Fig. 2, F and G). At 24 hours after partial hepatectomy, both WT and *cav1*$^{-/-}$ livers showed a similar increment of their triacylglycerol content, but at later times, significant differences between the WT and *cav1*$^{-/-}$ mice were observed. Thus, although *cav1*$^{-/-}$ mice were able to synthesize triacylglycerol to some extent, they could not store these lipids efficiently in lipid droplets. In agreement with an intracellular lipid imbalance, the expression of adipophilin (ADRP, the major component of hepatic lipid droplets and highly expressed in response to fatty acids during liver regeneration) was slightly but consistently higher in *cav1*$^{-/-}$ mice when compared to WT mice (Fig. 2H), although it was not detected in the fraction corresponding to purified lipid droplets (Fig. 2I). Thus, caveolin is required for efficient lipid droplet formation in regenerating hepatocytes, and the absence of lipid droplets at 48 hours after partial hepatectomy coincides with the increased mortality of *cav1*$^{-/-}$ mice beyond this point.

To examine the effect of caveolin-1 deficiency at the cellular level, hepatocytes from

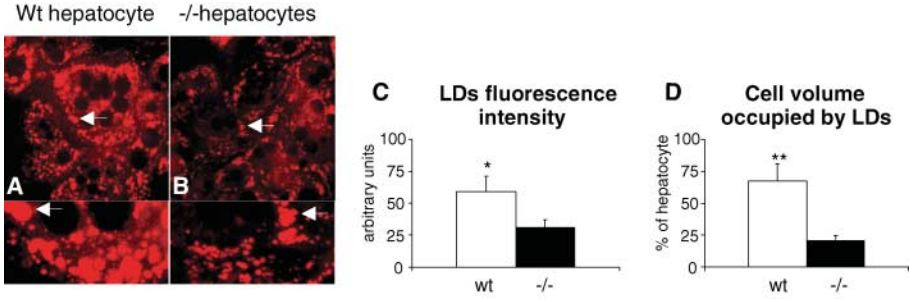

Fig. 3. Isolated *cav1*$^{-/-}$ hepatocytes show impaired lipid droplet accumulation. Hepatocytes were isolated from livers of WT mice (**A**) or *cav1*$^{-/-}$ mice (**B**) and allowed to attach on glass coverslips for 6 hours in a glucose-free medium supplemented with fatty acids. Cells were fixed and lipid droplet accumulation was analyzed by means of Nile Red fluorescence (**C**), and the percentage of the cytosol occupied by lipid droplets (**D**) was quantified in WT hepatocytes (white bars) and *cav1*$^{-/-}$ hepatocytes (black bars). Values are the result of three independent experiments. The statistical significance of differences between WT and *cav1*$^{-/-}$ mice (asterisks) was determined with Student's *t* test, $*P < 0.05$, $**P < 0.01$.

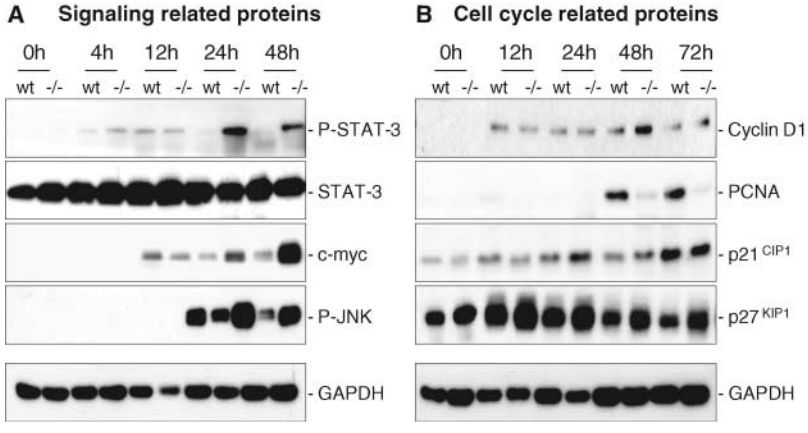

Fig. 4. Hyperactivation and cell cycle inhibition of *cav1*$^{-/-}$ hepatocytes after partial hepatectomy. The expression of markers corresponding to the acute phase response (**A**) or to the cell cycle machinery (**B**) in liver homogenates (40 μg) or for PCNA analyzed in isolated nuclei (20 μg) of WT and *cav1*$^{-/-}$ mice after partial hepatectomy is shown. Immunoblots are representative of at least three independent experiments. GAPDH, glyceraldehyde phosphate dehydrogenase.

WT and *cav1*$^{-/-}$ mice were isolated and treated with a combination of fatty acids for 6 hours. Hepatocytes growing on glass coverslips were stained with Nile Red (a neutral lipid probe) for detection of lipid droplets. As expected, fatty acids efficiently promoted the accumulation of enlarged lipid droplets in the cytosol of WT hepatocytes (Fig. 3A). In comparison, the intensity of Nile Red staining was significantly reduced in *cav1*$^{-/-}$ hepatocytes (Fig. 3, B and C). In addition, the mean volume of lipid droplets was 67.6% (±14.3%) of the cell cytosol in WT hepatocytes as compared to 20.5% (±4.9%) in *cav1*$^{-/-}$ cells (Fig. 3D). Hepatocytes isolated from WT and *cav1*$^{-/-}$ livers showed a similar uptake of fatty acids (fig. S1). When the expression of caveolin-1 was down-regulated by means of small interfering RNA in mouse embryonic fibroblasts obtained from WT mice, the accumulation of lipid droplets in cells expressing low levels of caveolin-1 was significantly reduced (fig. S2). In contrast, down-regulation of caveolin-2 in these cells did not affect the accumulation of lipid droplets (fig. S2). Thus, the inability of *cav1*$^{-/-}$ hepatocytes to accumulate lipid droplets during liver regeneration is caused by the lack of hepatic caveolin-1 rather than promoted by the absence of caveolin-1 in other tissues.

Hepatocytes without caveolin-1 do not efficiently accumulate triacylglycerol in lipid droplets and fail to regenerate. Caveolin is linked to numerous signaling processes, but the exact regulatory mechanisms are still unclear. We examined whether an impaired activation of the cells during the acute response may account for the lack of regeneration observed in *cav1*$^{-/-}$ mice. Hepatocyte activation after partial hepatectomy is promoted by two coordinated main signaling pathways: a cytokine-mediated pathway and a growth factor–mediated pathway. Binding of interleukin-6 (IL-6) to its receptor (IL-6 receptor) stimulates the Janus activated kinase (JAK-1), which in turn phosphorylates the signal transducer and activator of transcription 3 (STAT-3). Phosphorylated STAT-3 translocates to the nucleus to activate the transcription of target genes (such as c-*myc*). We examined the levels of phosphorylated STAT-3 and the expression of c-*myc* in liver homogenates. Twelve hours after partial hepatectomy, phosphorylation of STAT-3 was detected in both WT and *cav1*$^{-/-}$ mice (Fig. 4A). At later times, the levels of phospho–STAT-3 then decreased, as expected in WT mice livers, but STAT-3 remained phosphorylated in *cav1*$^{-/-}$ livers. Consistent with this finding, levels of c-*myc* were considerably higher in livers from *cav1*$^{-/-}$ mice. We also studied the growth factor–mediated signaling pathway. The hepatic growth factor (HGF) is considered to be an essential activator of the regeneration response of the liver. We evaluated HGF activity by visualizing the phosphorylation of its substrate, Jun N-terminal kinase (JNK). Phospho-JNK was detected in both WT and *cav1*$^{-/-}$ mice, but the levels of phosphorylated kinase were markedly higher in *cav1*$^{-/-}$ mice (Fig. 4A). Thus, although the acute phase response occurs as in WT mice, the signaling is more elevated and prolonged in *cav1*$^{-/-}$ livers.

We next evaluated the progression of hepatocytes through the cell cycle by studying specific proteins of the cell cycle machinery known to be regulated during liver regeneration (*11*). Expression of cyclin D, which is transcriptionally activated during the G_1 phase of the cell cycle, was observed in both WT and *cav1*$^{-/-}$ livers after 12 hours of partial hepatectomy (Fig. 4B). Although the proliferating cell nuclear antigen (PCNA, a marker for the S phase) was clearly observed at 48 to 72 hours in 95% of WT livers, its expression was not observed or was highly reduced in 80% of *cav1*$^{-/-}$ mice that survived at 72 hours. Although no differences were observed in the expression of the cell cycle inhibitor $p21^{CIP1}$, the amount of the inhibitor $p27^{KIP1}$ detected in *cav1*$^{-/-}$ livers was slightly but consistently higher when compared to WT mice. Thus, the livers of *cav1*$^{-/-}$ mice do not seem to progress correctly through the cell cycle. The impaired liver regeneration observed in *cav1*$^{-/-}$ mice did not appear to result in an increased rate of apoptosis; no differences in the activity of caspases measured in regenerating livers were observed (fig. S3).

Glucose can be the predominant energy substrate during liver regeneration, when sufficient levels are available during the immediate post-hepatectomy phase (*12*, *13*). The continuous infusion of glucose into partially hepatectomized rats prevents both the loss of glycogen and the deposition of lipid (*14*). Because the livers of *cav1*$^{-/-}$ mice do not correctly metabolize lipids after partial hepatectomy (Fig. 2), we hypothesized that the impaired liver regeneration showed by these mice might be due to the perturbation of lipid handling. If so, the

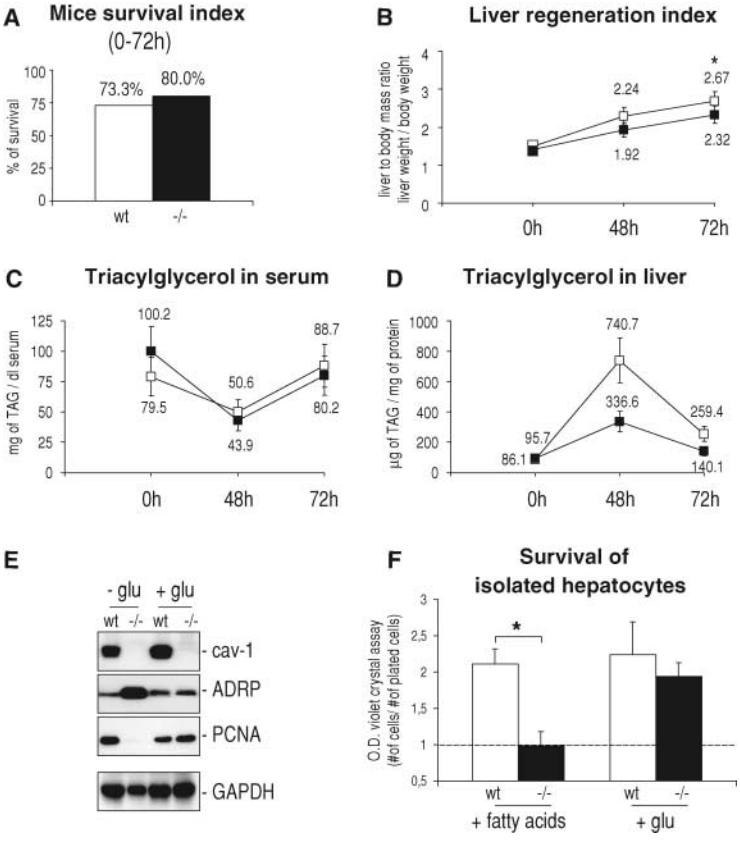

Fig. 5. The feeding of glucose reestablishes hepatocyte survival and cell cycle progression in *cav1*$^{-/-}$ mice. (**A**) Survival index after partial hepatectomy of glucose-treated *cav1*$^{-/-}$ mice (black bars) and WT mice (white bars). (**B**) Liver–to–body mass ratio corresponding to glucose-fed *cav1*$^{-/-}$ mice (black squares) and glucose-fed WT mice (white squares) after partial hepatectomy. (**C** and **D**) Triacylglycerol levels in serum (C) and liver homogenates (D) of glucose-fed WT mice (white squares) and glucose-fed *cav1*$^{-/-}$ mice (black squares) after partial hepatectomy. (**E**) The expression of caveolin-1 and ADRP in liver homogenates (40 µg) and of PCNA in isolated nuclei (20 µg). (**F**) Hepatocytes were isolated from livers of WT mice (white bars) and *cav1* $^{-/-}$ mice (black bars) and cultured for 48 hours in a medium supplemented with fatty acids or glucose. The number of living cells was determined by staining cell nuclei with crystal violet and is expressed with respect to the initial number of living hepatocytes. The statistical significance (asterisk) was determined with Student's *t* test, $*P < 0.05$. Each point and immunoblot represents the average value of at least four independent experiments. O.D., optical density.

treatment of animals with glucose before and during the regenerative process might allow liver regeneration in the *cav1*$^{-/-}$ mice. Thus, WT and *cav1*$^{-/-}$ mice were continuously supplied with 10% glucose in their drinking water for 60 hours before surgery and during the regeneration period afterward. Before partial hepatectomy, the ingestion of glucose-enriched water was approximately 10 ml per mouse per day (equivalent to 1 g of glucose per day). When *cav1*$^{-/-}$ mice were treated with glucose, the survival index at 72 hours after partial hepatectomy dramatically increased to reach values comparable to those of glucose-treated WT mice (80.0% for *cav1*$^{-/-}$ mice, $n = 26$ mice; 73.3% for WT, $n = 16$) (Fig. 5A). In WT mice treated with glucose, the liver regeneration index after 72 hours was 2.67% (±0.3), which, consistent with slightly delayed regeneration in glucose-fed rats (*15*, *16*), represents 45.3% (±5.1) of the original weight (Fig. 5B) (in contrast to 52.5% shown by WT mice that were not treated with glucose, Fig. 1D). Consistent with the decreased mortality of the *cav1*$^{-/-}$ mice, liver regeneration was rescued by glucose feeding. Glucose-fed *cav1*$^{-/-}$ mice showed a regeneration index of 2.32% (±0.4), which similarly to the WT glucose-fed mice represents 39.3% (±6.8) of the original liver weight. After partial hepatectomy, the levels of triacylglycerol in serum were similar to those shown by animals that were not treated with glucose. In contrast, in liver homogenate of glucose-fed animals, the level of triacylglycerol increased in both WT and *cav1*$^{-/-}$ mice (Fig. 5D). Although, as expected, no changes were observed in the expression of caveolin-1 (Fig. 5E), when treated with glucose, the expression of ADRP in *cav1*$^{-/-}$ animals was similar to that shown by WT mice (Fig. 5E). Treatment with glucose also rescued the inhibition of the cell cycle shown by *cav1*$^{-/-}$ mice (Fig. 4B). In that case, 87.5% of *cav1*$^{-/-}$ mice treated with glucose expressed high levels of PCNA 72 hours after partial hepatectomy (Fig. 5E). To examine the effect of glucose at the cellular level, hepatocytes from WT and *cav1*$^{-/-}$ mice were isolated and cultured in a glucose-free medium containing growth factors supplemented with a combination of fatty acids (0.5 mM palmitoleic acid and 0.5 mM oleic acid) or alternatively with glucose (4500 mg/l), and the number of cells was determined after 48 hours (number of living cells after 48 hours/number of living cells 6 hours after isolation) by staining of cell nuclei with a standard crystal violet measurement. In contrast to WT cells, *cav1*$^{-/-}$ hepatocytes did not survive in the presence of fatty acids, and a reduction in the number of cells was observed (Fig. 5F). In the presence of glucose, both WT and *cav1*$^{-/-}$ hepatocytes showed a similar index. Thus, the increased mortality and decreased liver regeneration in mice lacking caveolin-1 can be rescued by glucose addition, pinpointing the crucial role of caveolin-1 in lipid regulation during the regeneration process.

We have shown that caveolin is essential for liver regeneration. caveolin-1–deficient mice showed increased mortality and decreased liver regeneration after partial hepatectomy. In the absence of caveolin-1, hepatocytes did not accumulate lipid droplets, and this has important effects on other cellular processes such as cell signaling and cell division. As a result, regenerating *cav1*$^{-/-}$ hepatocytes showed atypical cell activation and did not entirely advance through the cell cycle. Because the treatment of *cav1*$^{-/-}$ mice with glucose increased mouse survival and reestablished progression of the cell cycle, we postulate that caveolin-1 has a crucial role in lipid regulation during the regeneration process. Thus, the S phase of the cell cycle may be metabolically regulated by the availability of lipid droplets or glucose. Although *cav1*$^{-/-}$ animals show a relatively mild phenotype, suggesting that other proteins may compensate for the lack of caveolins in certain cellular or functional contexts, caveolin-1 plays an essential role in the hepatocyte that becomes apparent only in response to liver injury.

References and Notes

1. N. Fausto, *Hepatology* **39**, 1477 (2004).
2. G. K. Michalopoulos, M. C. DeFrances, *Science* **276**, 60 (1997).
3. R. Taub, *Nat. Rev. Mol. Cell Biol.* **5**, 836 (2004).
4. E. A. Glende Jr., W. S. Morgan, *Exp. Mol. Pathol.* **8**, 190 (1968).
5. G. C. Farrell, *Hepatology* **40**, 1252 (2004).
6. T. V. Kurzchalia, R. G. Parton, *Curr. Opin. Cell Biol.* **11**, 424 (1999).
7. A. Pol *et al.*, *J. Cell Biol.* **152**, 1057 (2001).
8. A. Pol *et al.*, *Mol. Biol. Cell* **15**, 99 (2004).
9. M. Drab *et al.*, *Science* **293**, 2449 (2001).
10. S. Le Lay, T. V. Kurzchalia, *Biochim Biophys Acta* **1746**, 322 (2005).
11. J. H. Albrecht *et al.*, *Oncogene* **16**, 2141 (1998).
12. H. S. Lai, W. J. Chen, K. M. Chen, *J. Parenter. Enteral Nutr.* **16**, 152 (1992).
13. J. Simek, V. Chmelar, J. Melka, Z. Pazderka, Z. Charvat, *Nature* **213**, 910 (1967).
14. N. L. R. Bucher, R. A. Malt, *Regeneration of Liver and Kidney* (Little, Brown, Boston, 1971).
15. J. A. Caruana, D. A. Whalen Jr., W. P. Anthony, C. R. Sunby, M. P. Ciechoski, *Endocr. Res.* **12**, 147 (1986).
16. M. Holecek, J. Simek, *Exp. Pathol.* **33**, 257 (1988).

17. We thank A. Giménez, C. Claries, and O. Collazo from the Animal Facility (University of Barcelona) and the CORE facility (Hospital Clinic i Provincial de Barcelona). This work was supported by grants BMC2003-04754 and GEN2003-20662 to C.E. and BFU2005-01716 and GEN2003-20662 to A.P. [Ministerio de Educación y Ciencia (MEC), Spain] and a program grant from the National Health and Medical Research Council of Australia to R.G.P. A.P. and F.T. are supported by Ramón y Cajal Research Program (MEC). M.A.F. is supported by the postdoctoral fellowship program EX2005-0850 (MEC).

Supporting Online Material

www.sciencemag.org/cgi/content/full/313/5793/1628/DC1
Materials and Methods
Figs. S1 to S3
Table S1
References

2 June 2006; accepted 21 July 2006
10.1126/science.1130773

C-Terminal Signal Sequence Promotes Virulence Factor Secretion in *Mycobacterium tuberculosis*

Patricia A. DiGiuseppe Champion,[1,2] Sarah A. Stanley,[1,2] Matthew M. Champion,[3] Eric J. Brown,[2] Jeffery S. Cox[1,2]*

Mycobacterium tuberculosis uses the ESX-1/Snm system [early secreted antigen 6 kilodaltons (ESAT-6) system 1/secretion in mycobacteria] to deliver virulence factors into host macrophages during infection. Despite its essential role in virulence, the mechanism of ESX-1 secretion is unclear. We found that the unstructured C terminus of the CFP-10 substrate was recognized by Rv3871, a cytosolic component of the ESX-1 system that itself interacts with the membrane protein Rv3870. Point mutations in the signal that abolished binding of CFP-10 to Rv3871 prevented secretion of the CFP-10 (culture filtrate protein, 10 kilodaltons)/ESAT-6 virulence factor complex. Attachment of the signal to yeast ubiquitin was sufficient for secretion from *M. tuberculosis* cells, demonstrating that this ESX-1 signal is portable.

Proteins are sorted for translocation across cellular membranes through recognition of signal sequences (*1*, *2*). In prokaryotes, most proteins are secreted through the general secretion pathway, which recognizes N-terminal signal peptides (*3*). Additionally, Gram-negative pathogenic bacteria use specialized secretion machines to secrete virulence determinants during infection (*4*, *5*).

Mycobacterium tuberculosis does not have recognizable homologs of these specialized secretion systems. Instead, the ESX-1 system (ESAT-6 system-1) is required for controlling host-cell response to infection (*6*–*8*). ESX-1 is

[1]Department of Microbiology and Immunology, [2]Program in Microbial Pathogenesis and Host Defense, University of California, San Francisco, 600 16th Street, Campus Box 2200, San Francisco, CA 94143–2200, USA. [3]Applied Biosystems, 353 Hatch Drive, Foster City, CA 94404, USA.

*To whom correspondence should be addressed. E-mail: Jeffery.Cox@ucsf.edu